Preequilibrium (p, p') measurements and calculations for ^{90}Zr and neighboring nuclei for incident energies up to 200 MeV

W. A. Richter, A. A. Cowley, G. C. Hillhouse,* J. A. Stander, J. W. Koen, and S. W. Steyn
University of Stellenbosch, Stellenbosch 7600, South Africa

R. Lindsay and R. E. Julies
University of the Western Cape, Bellville 7530, South Africa

J. J. Lawrie and J. V. Pilcher
National Accelerator Centre, Faure 7131, South Africa

P. E. Hodgson
Nuclear Physics Laboratory, Department of Physics, University of Oxford, Oxford OX1 3RH, United Kingdom
(Received 12 August 1993)

Double-differential cross sections have been measured for inclusive (p, p') reactions on targets of ^{89}Y, ^{90}Zr, and the even-mass Mo isotopes from $A = 92$ to 98 at incident proton energies of 120, 160, and 200 MeV. Comparisons are made with calculations based on the statistical multistep direct theory of Feshbach, Kerman, and Koonin. In general it is found that the theory gives a good description of the angular distributions. Possible explanations for the deviation of the predicted cross sections from experiment at very low and very high excitation energies of the residual nucleus are given.

PACS number(s): 24.60.Gv, 25.40.−h

I. INTRODUCTION

In a previous paper [1] a remarkable agreement with experiment was obtained at incident energies of 80 and 120 MeV for the ^{90}Zr(p, p') angular distribution calculated with the multistep direct reaction code of Bonetti and Chiesa [2], which is based on the statistical multistep direct reaction theory of Feshbach, Kerman, and Koonin (FKK) [3]. These results prompted the present further investigation to test the validity of the FKK theory for the reaction ^{90}Zr(p, p') at higher incident energies of up to 200 MeV, and to explore, in particular, the trend of the quality of the agreement between theory and experiment for that target nucleus. In addition, the (p, p') experiment on ^{90}Zr at incident energies of 160 and 200 MeV was supplemented by measurements on targets of even-mass Mo isotopes from A=92 to 98, as well as ^{89}Y at the same incident energies. This enabled comparisons for neighboring nuclei to be made. Additional measurements at an incident energy of 120 MeV were also carried out on the latter nuclei to complete the data set for the three incident energies 120, 160 and 200 MeV.

Recently, it has been shown [4] that the FKK theory can be successfully applied to predict direct-emission spectra of protons induced by incident protons at energies up to 200 MeV for three targets ranging in mass number from 58 to 197. However, in the present work the FKK theory is compared with experimental data between 120 and 200 MeV in a more limited mass range 89–98 in order to investigate further the variations with incident energy and target mass, and possible odd-even and shell effects.

In Sec. II experimental details are discussed. Some details of the calculations are described in Sec. III. Section IV A consists of a comparison between the theoretical and experimental angular distributions of the continuum spectra at selected emission energies, and in Sec. IV B target-mass and isotopic trends are investigated. Multistep compound contributions are considered in Sec. IV C, and in Sec. IV D a comparison of the effective interaction strength V_0 is made with previous analyses. Finally, in Sec. V, a summary of the main conclusions is given.

II. EXPERIMENTAL DETAILS

The experiment was performed at the cyclotron facility of the National Accelerator Centre, Faure. Accounts of the equipment and experimental technique have been presented in Refs. [5–7]. The targets used and target thicknesses are summarized in Table I. Target thicknesses were determined by comparing the measured energy loss of alpha particles from a ^{228}Th source with calculated values using stopping-power tables of Ziegler [8]. Whereas the absolute thickness determination is only accurate to within 8% due to uncertainties in the energy-loss calculation, relative errors are less than 3%. The

*Present address: University of the Western Cape, Bellville 7530, South Africa.

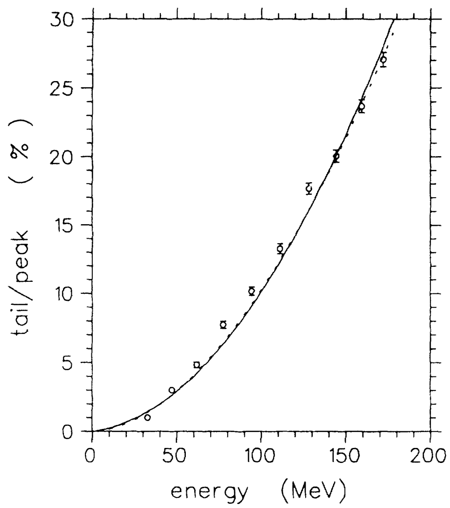

FIG. 1. Experimental tail-to-peak ratios compared with calculated values from Eq. (1) (solid line) and from the form given by Green *et al.* [9] (dotted line).

target uniformity is typically 1%/mm.

In our previous experiments on inclusive (p,p') reactions, corrections for the reaction tail and efficiency of the NaI detectors followed the procedure described by Green *et al.* [9], where they assume that the reaction tail increases linearly from zero at zero energy to a maximum at the full energy of the detected particle. Since we now require more accurate tail corrections, we attempted to improve the correction by measuring the shape of the reaction tail for proton energies up to 200 MeV.

These reaction tail measurements involved the coincident observation of p-p elastic scattering at an incident-proton energy of 200 MeV using a 1.5 mg/cm^2 polyethylene target. A primary detector telescope, covering an angular range from 20° to 65° in 5° steps, detected elastically scattered protons with energies ranging from 173 MeV to 33 MeV. The coincident observation of the recoil proton in a secondary detector telescope, mounted at the appropriate angles for p-p scattering, served to minimize interference from reaction products from carbon. The detector telescopes were identical to those used in the

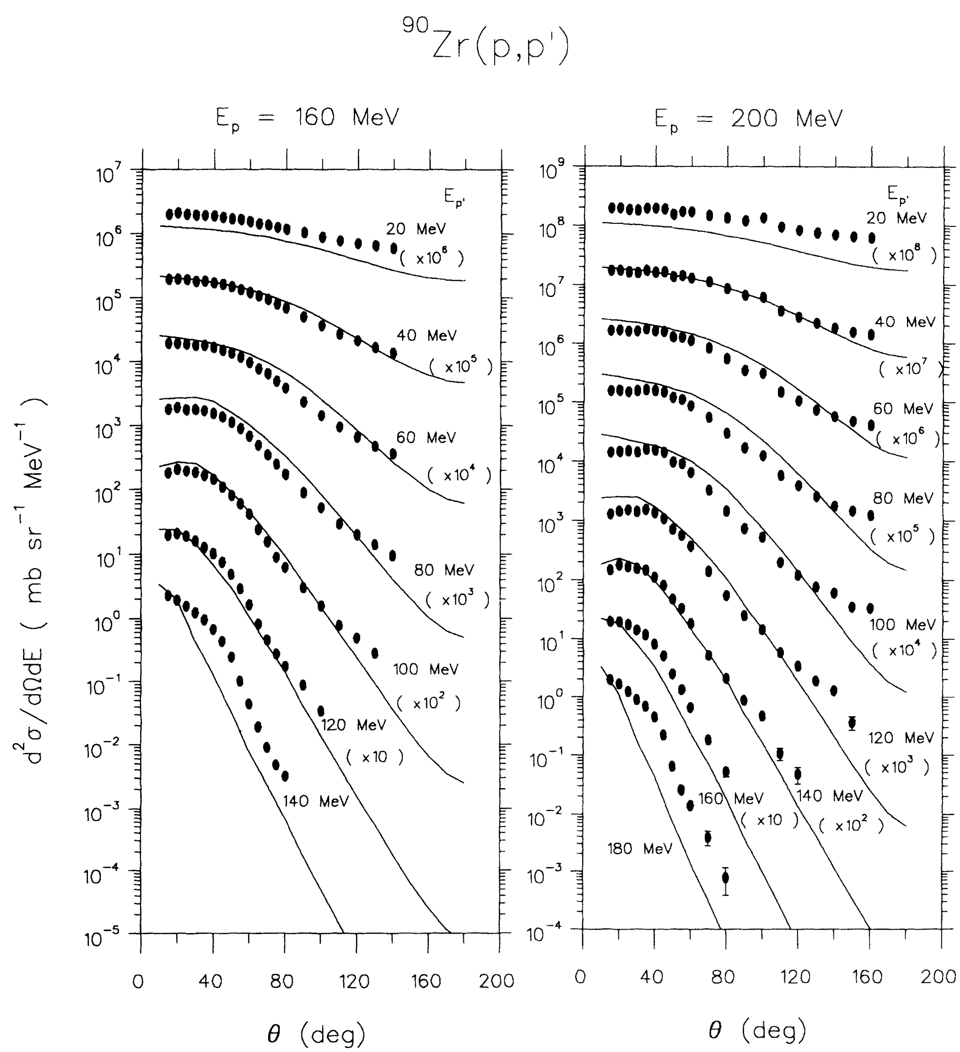

FIG. 2. Experimental angular distributions for ^{90}Zr(p,p') at various incident energies E_p and emission energies $E_{p'}$. Statistical error bars are shown where these exceed the symbol size. The curves are results of MSD calculations. Results are multiplied by the indicated factors for display.

TABLE I. Target thicknesses in mg cm^{-2}.

^{89}Y	^{90}Zr	^{92}Mo	^{94}Mo	^{96}Mo	^{98}Mo
11.2	10.1	1.21	1.17	0.94	1.05

inclusive (p,p') measurements, and standard coincidence techniques were used.

During analysis of the data, a narrow gate in the particle-identification spectrum of the secondary telescope selected recoil protons at the full energy for elastic p-p scattering, while the corresponding gate in the primary telescope included protons of all energies up to and including the full energy peak. An additional gate in a spectrum of E_1 (primary-telescope energy) versus E_2 (secondary-telescope energy) served to reduce background from the reaction $^{12}\mathrm{C}(p,2p)$. Extracted energy spectra for the primary telescope were normalized to the same number of counts in the elastic peak.

The number of counts in the reaction tail T, expressed as a function of the observed energy E and the peak energy E_p, were parametrized in terms of Legendre polynomials P_i of odd order, and can be written in the form

TABLE II. Legendre polynomial coefficients from Eq. (1) fitted to the experimental data.

a_1	a_3	a_5	a_7
1.71×10^{-5}	-1.39×10^{-3}	-7.51×10^{-4}	-7.47×10^{-4}

$$T(E,E_p) = E_p a_1 P_1(E/E_p) + \sum_{i=3}^{7} a_i P_i(E/E_p). \qquad (1)$$

The multiplication factor E_p in the first term was included to reproduce a slope that is independent of the peak energy, as suggested by the experimental data.

The constants a_i obtained in a simultaneous least-squares fit to the data are given in Table II, where values have been normalized to a yield of unity in the full energy peak. From Eq. (1), the tail to peak ratio is given by

$$f(E_p) = (8.55E_p^2 + 157E_p) \times 10^{-6}. \qquad (2)$$

In Fig. 1 this is compared with experimentally determined values from the present study and with the functional form of Green *et al.* [9]. The improved form of the

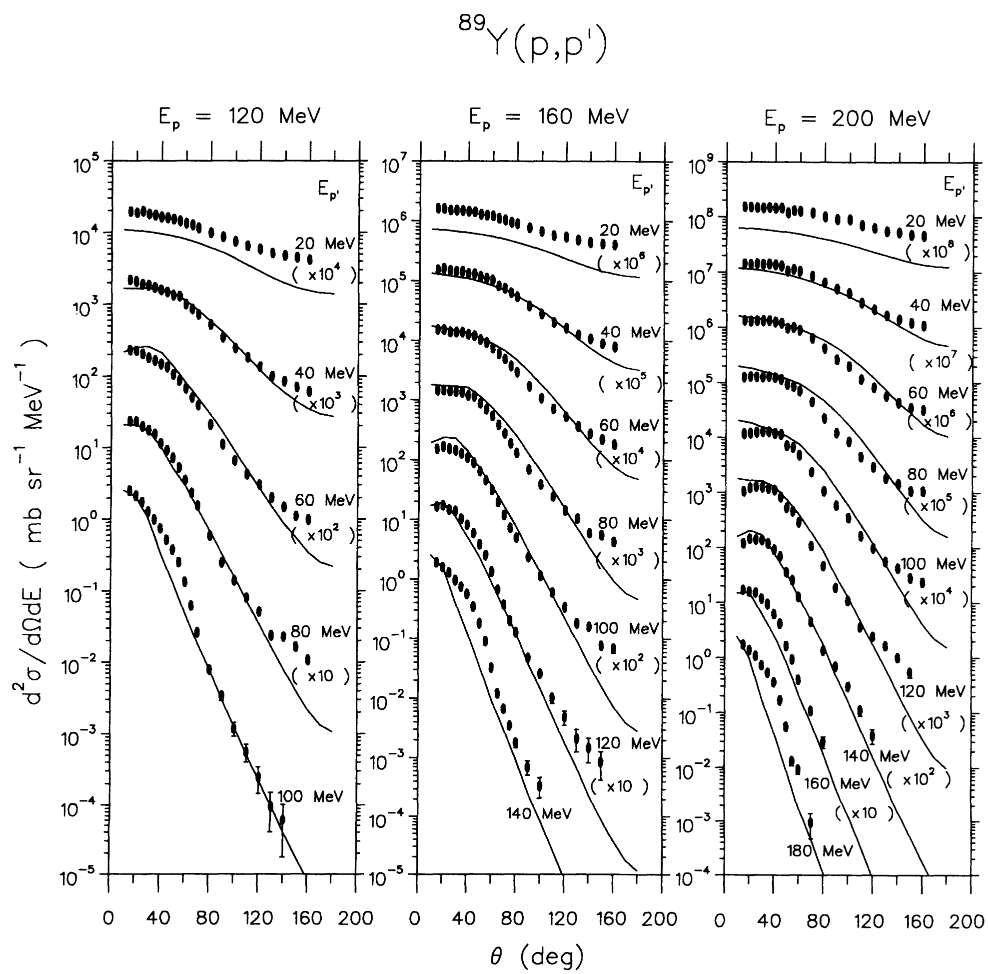

FIG. 3. Experimental angular distributions and MSD calculations for $^{89}\mathrm{Y}(p,p')$. See also caption to Fig. 2.

reaction tail has a negligible effect for excitation energies of more than 20 MeV, and also at large scattering angles where the yield from elastic scattering is low compared to the continuum cross section.

III. CALCULATIONAL DETAILS

The FKK theory [3] of multistep direct emission has been described frequently, and a brief summary of the formalism may be found in Ref. [4]. The calculations were performed with the program of Bonetti and Chiesa [2]. Although it is beyond the scope of the present work to study the numerical accuracy of the computer code, we have nevertheless investigated the integration technique used. This was motivated by the results of Koning and Akkermans [10], who calculated cross sections for the FKK theory with their own program which (depending on the step in the multistep chain) differed by up to an order of magnitude from those of the Bonetti code. Koning and Akkermans ascribed these differences to their use of an alternate, more reliable, integration technique. Therefore, to explore this further, we have performed a calculation in which the rectangular integration in the program of Bonetti was replaced with the Simpson technique. Our results indicate differences which are significantly smaller than those reported in Ref. [10] and which are typically less than ten to twenty percent of the original values. Consequently we conclude that the discrepancies found by Koning and Akkermans are not likely to be primarily associated with the integration technique.

A level density parameter a proportional to the mass number A of the target nucleus has been assumed, as in Ref. [4], viz. $a=A/8.5$ MeV^{-1}. In the calculations, a value must also be chosen for the spin cutoff parameter σ, and this was selected to be consistent with our previous work [1, 4]. Our values are smaller than those given by $\sigma = \sqrt{0.24nA^{2/3}}$ (where n is the exciton number, which is equal to the number of particles and holes), as suggested in Ref. [11]. A finite range (1 fm) Yukawa potential was used for the two-body effective interaction, of which the strength V_0 is adjusted to best reproduce the data. The calculated cross sections were normalized by choosing values of V_0 to give the best overall χ^2 agreement with the experimental angular distribution at an emission energy corresponding to half the incident energy. As the effective interaction enters at each step of the multistep chain, the final cross section for the nth step is proportional to $(aV_0)^{2n}$. This is because both V_0

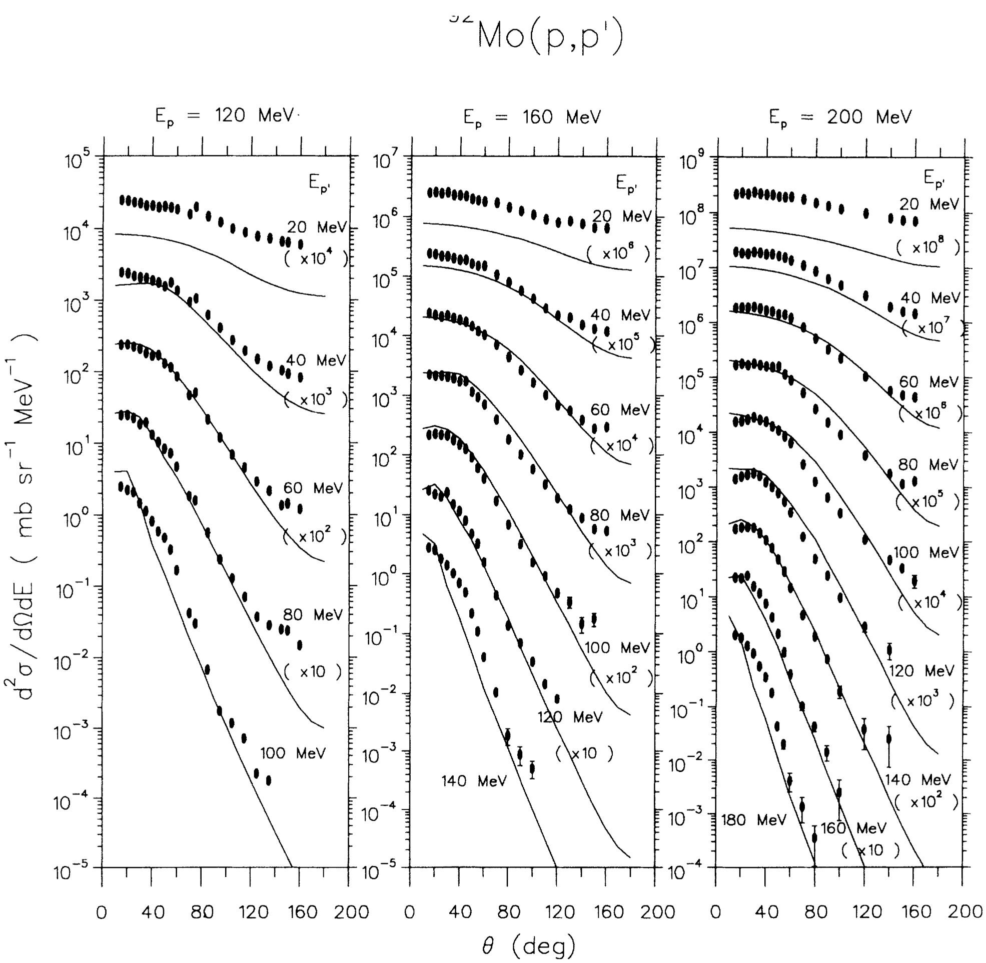

FIG. 4. Experimental angular distributions and MSD calculations for ^{92}Mo(p,p'). See also caption to Fig. 2.

and a enter quadratically in the distorted-wave Born approximation (DWBA) matrix elements contained in the FKK theory. Hence the level-density parameter and the effective interaction strength have to be considered simultaneously when parameters of the calculations are fixed *a priori*.

The maximum number of partial waves $L_{\max}$ used in the DWBA calculations varied between 30 (for incident energy $E_p = 120$ MeV) and 70 (for incident energy $E_p = 200$ MeV), and the number of steps employed in the calculations varied from 5 for the lower to 6 for the higher incident energies.

IV. RESULTS AND DISCUSSION

A. Comparison of theoretical and experimental angular distributions

The comparison between the FKK theory and the data for ^{90}Zr at incident proton energies of 160 and 200 MeV is shown in Fig. 2 for a range of energies of the emitted proton (or excitation energy of the residual nucleus $U = E_p - E_{p'}$, assuming one-particle emission). Note that the experimental data in Fig. 2, and also subsequent figures (e. g. in Figs. 3–7), are given in the laboratory system. Although the calculations are specified in the c.m. system, the effect of conversion of the measured data (under the assumption of one-particle emission) would only be comparable to the influence of the combined experimental uncertainties for the heavy targets used. Thus, the experimental data are retained in the laboratory system in preference to a model-dependent transformation, but this does not compromise the comparison between the measurements and the theoretical calculations.

In general, a good correspondence between experiment and the FKK theory is obtained at both incident energies in Fig. 2, although the quality of the agreement is not as good as that at the lower incident energies of 80 and 120 MeV [1]. It is evident that the FKK theory underestimates the cross sections at the lowest and highest excitation energies. For low excitation, it has been previously suggested [4] that the discrepancy could be due to multiparticle emission, in this case of predominantly two-proton or proton-neutron emission, which is not included in the FKK theory. The fact that this discrepancy appears to become more prominent at higher incident energy is also consistent with such an interpretation. In addition, some effects due to collective excitations may still contribute to the cross section at these excitation energies.

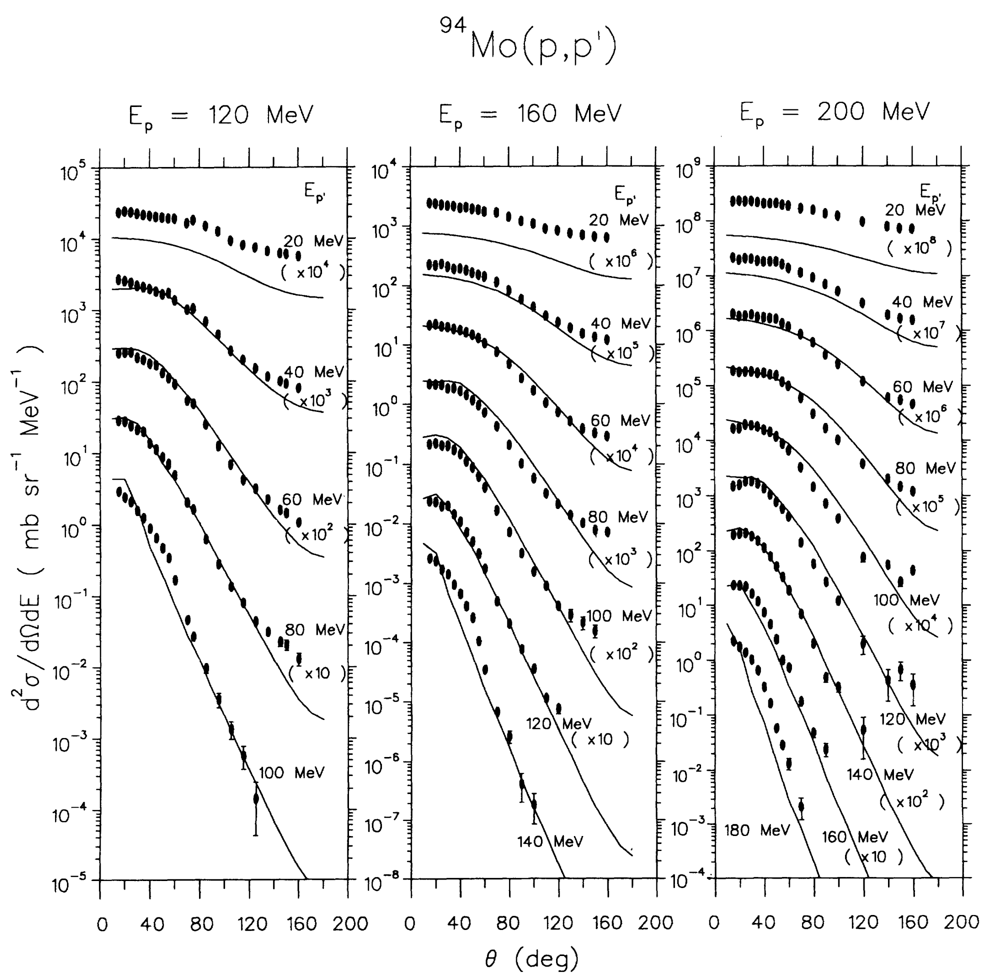

FIG. 5. Experimental angular distributions and MSD calculations for ^{94}Mo(p,p'). See also caption to Fig. 2.

The angular distributions for the targets ^{89}Y, and the even-mass isotopes of Mo from $A = 92$ to 98, at proton incident energies of 120, 160, and 200 MeV are given in Figs. 3 to 7. On the whole, the FKK calculations reproduce the angular distributions for all the targets quite well. It is significant that for the lower incident energies the general agreement extends over more than three orders of magnitude for the highest emission energies shown. However, as was already mentioned for ^{90}Zr, some discrepancies between experiment and theory are also evident for these other targets at the lowest and highest excitation energies, irrespective of the incident energy. In addition to the multiparticle emission already mentioned, and collective effects at low excitation energy, a variety of other factors may also be important. Examples are contributions from secondary processes or deficiencies in the global optical potential [12] used at these energies.

Part of the discrepancy between theory and experiment may also be due to transitions from sequences of states of increasing complexity, corresponding to the multistep direct part (P chain), to the similar series for the multistep compound component (Q chain). These transitions can give multistep compound contributions to the cross section even at high incident energies where the feeding of the Q chain from the entrance channel is negligible. Studies at lower incident energies have shown that the total statistical contribution to the cross section is somewhat greater than would be expected from the entrance channel width, suggesting the presence of later P to Q chain transitions [13, 14]. Such transitions could give appreciable multistep compound contributions to the cross section even at high energies where the Q-chain entrance channel width has become very small. This will be discussed further in Sec. IV C.

B. Systematic target-mass and isotopic trends

A direct comparison between the experimental double-differential cross sections $\frac{d^2\sigma}{d\Omega dE}$ for the various target nuclei for specific emission energies is shown in Figs. 8 and 9. Representative nuclei are shown. Clearly the cross section increases as the target is changed from ^{89}Y to ^{90}Zr, and again to ^{92}Mo, and this trend is observed at excitation energies as low as 20 MeV (emission energy: 140 MeV), as well as at the highest displayed excitation energy of 140 MeV (emission energy: 20 MeV) as shown in Fig. 8. The Mo isotopic trend is manifested less clearly, but there does seem to be a decreasing tendency in the cross section values with increasing mass at small emis-

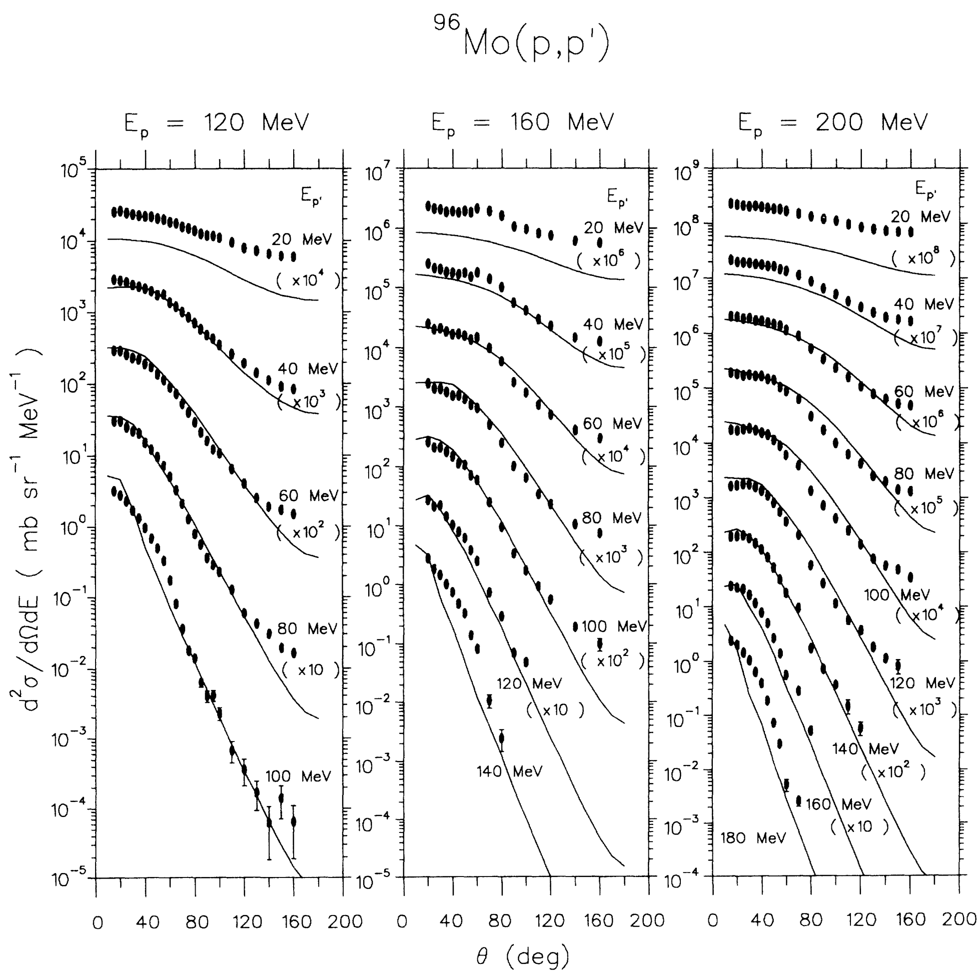

FIG. 6. Experimental angular distributions and MSD calculations for ^{96}Mo(p,p'). See also caption to Fig. 2.

sion energies, as shown in Fig. 9. Note that ^{92}Mo (not displayed in Fig. 9, but only shown in Fig. 8 for clarity of presentation) has roughly the same cross sections as those of ^{94}Mo (only included in Fig. 9).

The angle-integrated differential cross sections $\frac{d\sigma}{dE}$ are shown as a function of emission energy in Fig. 10. Again, a trend similar to that indicated by the double-differential cross sections is found. It should be noted that the relative differences in cross section observed for the different target masses are reliable, as may be inferred from the way in which the relative target thicknesses were determined, which was detailed in Sec. II. However, an overall systematic uncertainty exists.

Our findings regarding the mass dependence are different from those of Watanabe *et al.* [15] for the same reactions studied at an incident energy of 12 to 18 MeV. In their work, the preequilibrium cross section appears to be free of shell and odd-even effects.

In order to investigate this variation in cross section with target mass, FKK calculations were performed. In these calculations, the strength of the effective interaction was fixed at a constant value. Representative examples are shown in Fig. 11 for the isotopes of Mo. Although the calculations do display variations in cross section comparable in magnitude to those observed experimentally, the target-mass dependence was not reproduced systematically. We conclude that our calculations do not enable us to infer a definite origin of the mass dependence, and that the observed phenomenon probably results from detailed differences in the targets which are not treated explicitly in our calculational procedure.

We have considered a $(N-Z)/A$ dependence of the effective interaction, which might be similar to that of the real part of the proton optical potential [16] V_p, viz.

$$V_p \approx 50 + 20(N-Z)/A, \tag{3}$$

but the inclusion of such a term would not reproduce the observed variation of cross section with target nucleus. Deviations of the level-density parameter a from the assumed target-mass dependence are also unlikely to account for the trend observed in the experiment. In fact, the level densities listed in, e.g., Ref. [17] also suggest a monotonic increase of the values with target mass for the range under consideration.

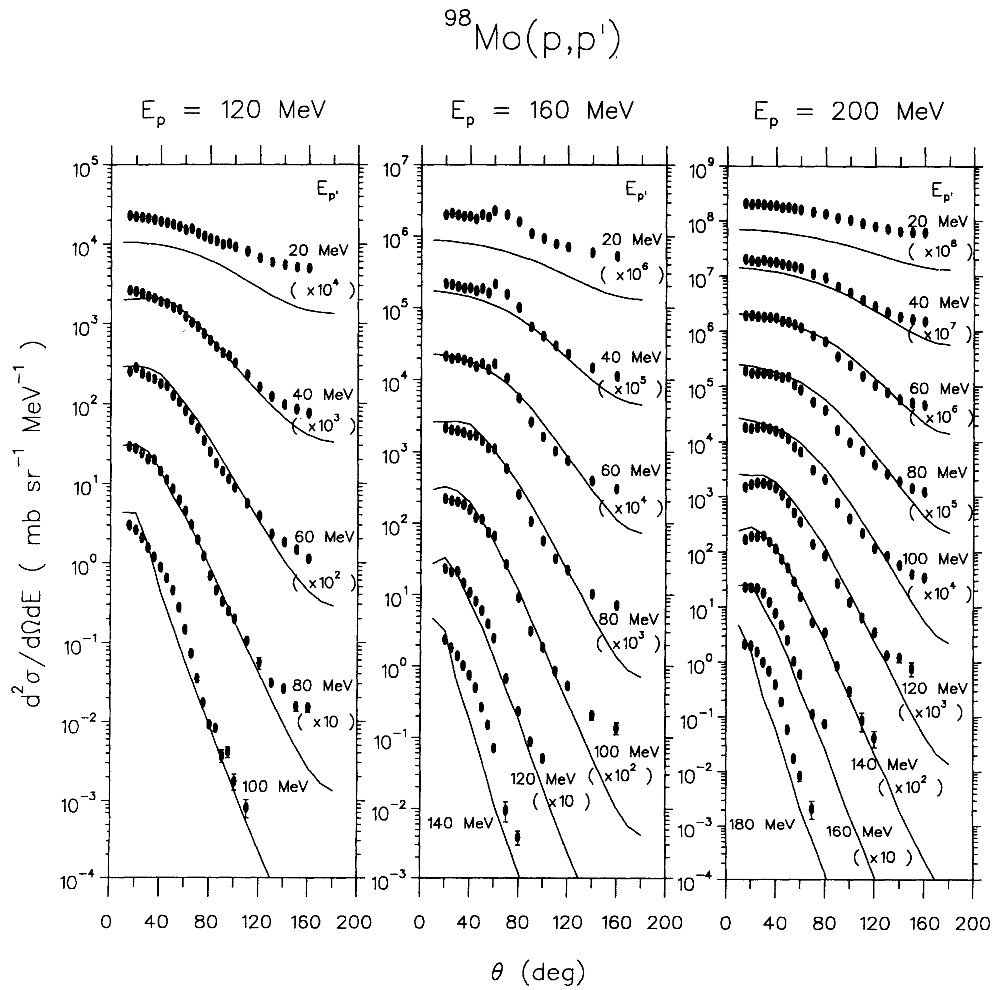

FIG. 7. Experimental angular distributions and MSD calculations for ^{98}Mo(p,p'). See also caption to Fig. 2.

C. Multistep compound contributions

At the lowest emission energy (20 MeV), the theoretical calculations predict cross sections which are consistently lower than the experimental values for all target nuclei, irrespective of incident energy. It is noticeable that with an increase to only 40 MeV in emission energy, the agreement is quite satisfactory. This suggests that a multistep compound reaction mechanism (plus compound-nucleus emission, which could contribute at an emission energy as low as 20 MeV) may explain at least part of the discrepancy at the lowest emission energy.

A convenient way in which multistep compound contributions may be eliminated for the purpose of comparison between calculated and experimental cross section values is to construct the quantity [18]

$$\begin{aligned}\sigma_{\text{diff}} &\equiv \sigma(\theta) - \sigma(\pi - \theta)\\ &= \sigma_D(\theta) + \sigma_C(\theta) - \sigma_D(\pi-\theta) - \sigma_C(\pi-\theta)\\ &= \sigma_D(\theta) - \sigma_D(\pi-\theta), \end{aligned} \tag{4}$$

where $\sigma_D(\theta)$ and $\sigma_C(\theta)$, respectively, represent the multistep direct and multistep compound (which includes preequilibrium as well as compound-nucleus emission)

TABLE III. Values of the strength of the effective interaction V_0 obtained from the present work (based on a Yukawa potential of range 1 fm). Values from Ref. [1] are also indicated by asterisk.

Target	E_p (MeV)	V_0 (MeV)	a	σ
^{90}Zr	80*	23	10.6	2.3
	120*	18	10.6	2.3
	160	15	10.6	2.3
	200	15	10.6	2.3
^{89}Y	120	18	10.5	2.3
	160	16	10.5	2.3
	200	15	10.5	2.3
^{92}Mo	120	19	10.8	2.5
	160	18	10.8	2.5
	200	16	10.8	2.5
^{94}Mo	120	19	11.1	2.5
	160	16	11.1	2.5
	200	15	11.1	2.5
^{96}Mo	120	19	11.3	2.5
	160	18	11.3	2.5
	200	16	11.3	2.5
^{98}Mo	120	19	11.5	2.5
	160	18	11.5	2.5
	200	16	11.5	2.5

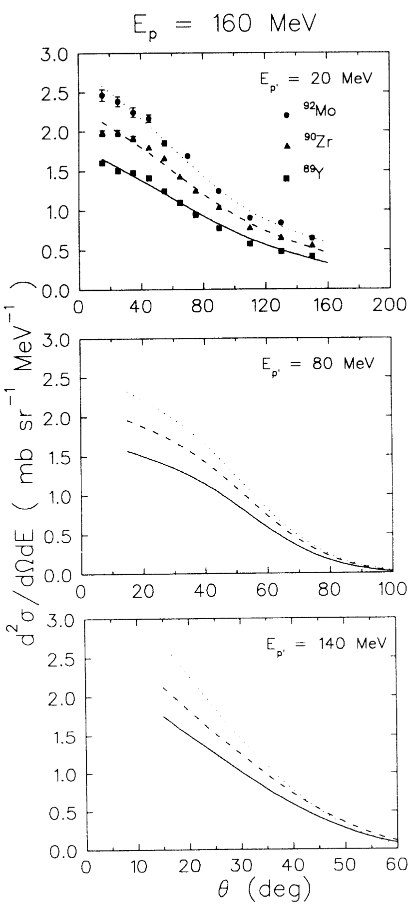

FIG. 8. Experimental inclusive (p,p') cross sections for $E_p = 160$ MeV as a function of scattering angle for various selected ejectile energies and ^{89}Y, ^{90}Zr and ^{92}Mo targets. For clarity of representation, only lines which are guides to the eye to the selected data from Figs. 2–4 are shown.

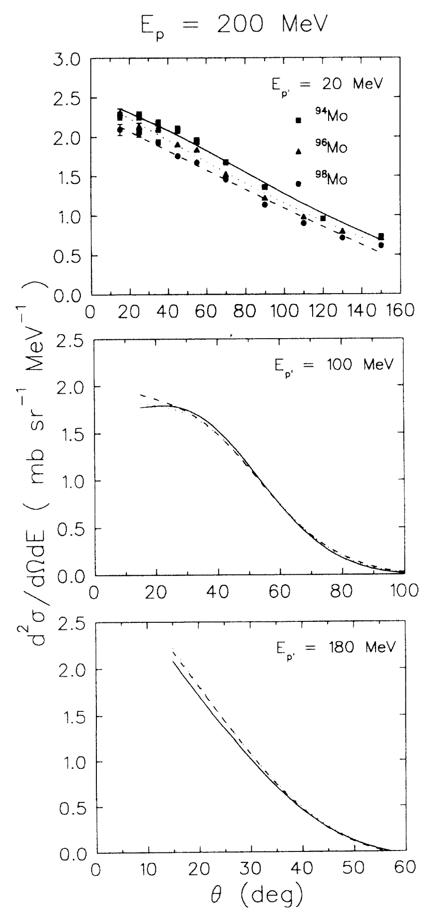

FIG. 9. Experimental inclusive (p,p') cross sections for $E_p = 200$ MeV as a function of scattering angle for various selected ejectile energies and ^{94}Mo, ^{96}Mo and ^{98}Mo targets. For clarity of representation, only lines which are guides to the eye to the selected data from Figs. 5–7 are shown.

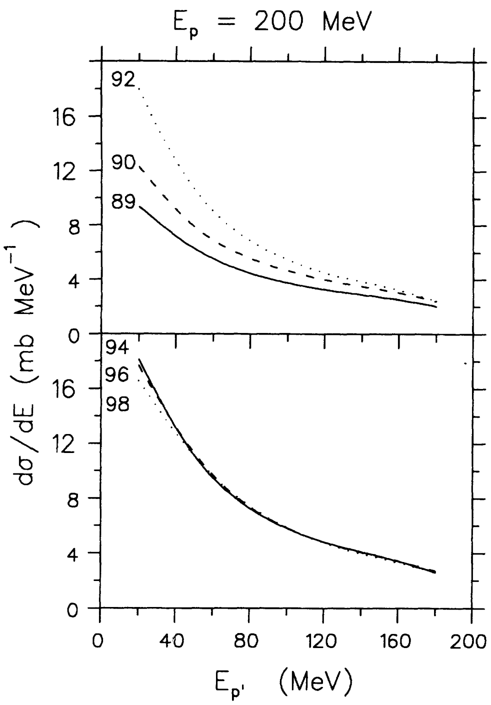

FIG. 10. Angle-integrated double-differential cross sections. The mass numbers of the target nuclei are indicated.

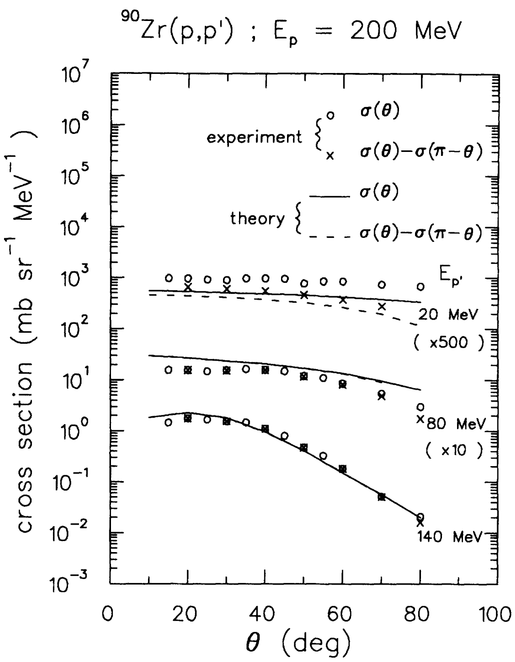

FIG. 12. Comparison of complementary-angle difference cross sections and double-differential cross sections for ^{90}Zr at $E_p = 200$ MeV.

cross sections $\frac{d^2\sigma}{d\Omega dE}$. The scattering angle is denoted by θ. In Fig. 12, the value of $\sigma_{\rm diff}$ (which now includes only the multistep direct component) is compared with $\sigma(\theta)$ for representative cases. At high emission energies where $\sigma_D(\pi-\theta)$ is small compared to $\sigma_D(\theta)$, and $\sigma_C(\theta)$ is expected to be negligible,

$$\sigma_{\rm diff} \approx \sigma(\theta) \tag{5}$$

approximately to within the experimental error bars for both the theoretical and experimental cross sections, thus confirming the expectation. At the lowest emission energy, where these considerations should no longer hold, the effect of constructing the difference cross section $\sigma_{\rm diff}$ is very noticeable.

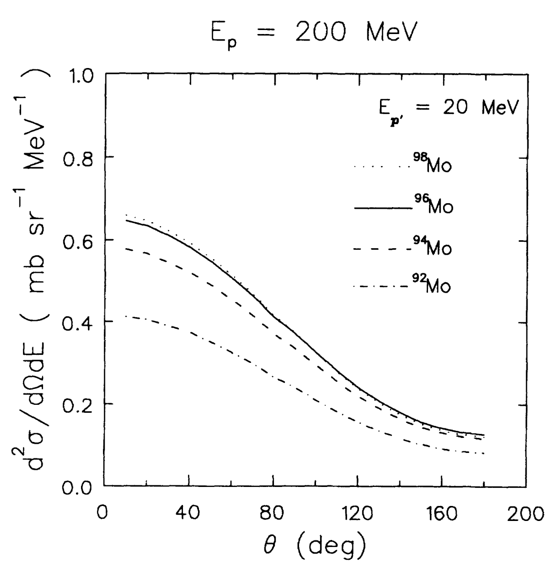

FIG. 11. Calculated double-differential cross sections as a function of scattering angle for an incident energy of 200 MeV and outgoing energy of 20 MeV with the effective interaction strength V_0 fixed at 16 MeV.

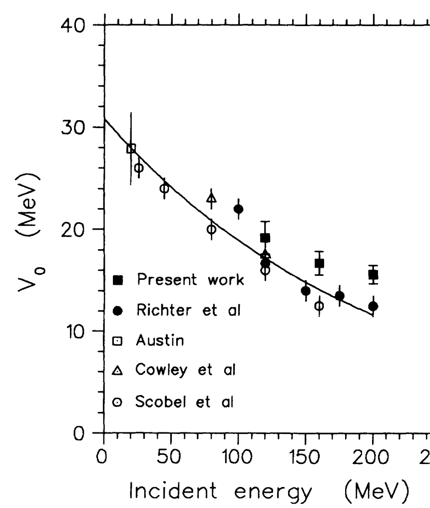

FIG. 13. The effective interaction strength V_0 as a function of incident energy. The values are compared with those of Richter *et al.* [4], Austin [20], Cowley *et al.* [1], and Scobel *et al.* [19]. Strengths displayed for the present work are averaged values at each incident energy. The solid curve indicates the normalized energy dependence of the optical potential, as described in the text.

As may be seen in Fig. 12, for the lowest emission energy, the theoretical values of σ_{diff} are still lower than the corresponding experimental values, but only by $\sim$ 30%. Furthermore, the experimental and theoretical angular distributions are in excellent shape agreement for this emission energy.

The 30% deficiency in absolute cross section of the multistep direct emission theory for the lowest emission energy is not very large, especially if we keep in mind (as we will see in the next section) that the strength of the effective interaction is energy dependent—a fact which we do not take into account in the calculations, due to questions regarding the exact energy dependence and how this should be accurately treated in the successive scatterings. The approximate inclusion of this energy dependence in Ref. [4] indicates that it would increase the cross section at low emission energies, as needed.

Therefore, accepting that a 30% difference between the experimental and theoretical angular distribution does not indicate a serious deficiency in the model calculations, it is possible to deduce the multistep compound contribution by renormalizing the theoretical cross sections to eliminate the difference, and then subtracting the normalized values from the experimental quantities. In this way, multistep compound contributions of $\sim$ 20% at forward angles to $\sim$ 60% at backward angles are extracted for the lowest emission energy. This procedure of extracting the multistep compound contribution relies on the assumption that the calculated shape of the multistep direct part is correct. As we have seen this is true for the higher emission energies, and it is consequently likely to be a reasonable assumption for the lowest emission energy.

D. The effective interaction V_0

It is of interest to compare our values of the effective interaction strength V_0 (Table III) with the results of previous analyses in Fig. 13. These calculations all used harmonic-oscillator wave functions for the bound nucleons, optical-model wave functions for the emitted nucleons, and Yukawa two-body interactions with a range of 1 fm. The scatter in values of V_0 is partly due to the differences in the analyses, but clearly the energy dependence of the effective interaction manifests itself prominently. Thus the trend with incident energy found in this work is consistent with those of previous studies [1, 4, 19, 20], and it is also in agreement with the energy dependence of the optical model (shown as the curve in Fig. 13) as discussed previously, for example, in Ref. [4].

V. SUMMARY AND CONCLUSIONS

It has been shown that the statistical multistep direct theory of Feshbach, Kerman, and Koonin reproduces experimental inclusive (p,p') continuum-angular distributions of the selected target nuclei reasonably well, but discrepancies are observed at the lowest and highest emission energies for all cases which were studied. Although we have not performed calculations appropriate to two-particle knockout in this study, it appears that contributions from such a process, which was investigated in Ref. [4], might explain the differences between the theoretical calculations and the experimental data at high emission energies. At the lowest emission energy studied, on the other hand, an appreciable contribution of multistep compound emission is inferred, with only a relatively small ($\sim$ 30%) discrepancy between multistep direct theoretical and experimental cross sections. At all other emission energies, the multistep compound component is negligible.

The experimental absolute cross sections show a systematic trend with target (Z and A). However, we are not able to identify the origin of this phenomenon, as the theoretical cross sections are sensitive to details of the calculations to the same extent as the differences observed experimentally.

In conclusion, therefore, the calculations based on the multistep direct theory are in general satisfactory, and the reasons for deficiencies at the highest and lowest emission energies are understood. However, there is clearly a need to refine the theory to include two-particle emission, especially at higher incident energies.

[1] A. A. Cowley, A. van Kent, J. J. Lawrie, S. V. Förtsch, D. M. Whittal, J. V. Pilcher, F. D. Smit, W. A. Richter, R. Lindsay, I. J. van Heerden, R. Bonetti, and P. E. Hodgson, Phys. Rev. C **43**, 678 (1991).

[2] R. Bonetti and C. Chiesa, MSD code, University of Milan, unpublished.

[3] H. Feshbach, A. Kerman, and S. Koonin, Ann. Phys. (N.Y.) **125**, 429 (1980).

[4] W. A. Richter, A. A. Cowley, R. Lindsay, J. J. Lawrie, J. V. Pilcher, S. V. Förtsch, R. Bonetti, and P. E. Hodgson, Phys. Rev. C **46**, 1030 (1992).

[5] J. V. Pilcher, A. A. Cowley, D. M. Whittal, and J. J. Lawrie, Phys. Rev. C **40**, 1937 (1989).

[6] A. A. Cowley, S. V. Förtsch, J. J. Lawrie, D M. Whittal, F. D. Smit, and J. V. Pilcher, Z. Phys. A **336**, 189 (1990).

[7] S. V. Förtsch, A. A. Cowley, J. J. Lawrie, D. M. Whittal, J. V. Pilcher, and F. D. Smit, Phys. Rev. C **43**, 691 (1991).

[8] J. F. Ziegler, in *The Stopping and Range of Ions in Matter; Helium: Stopping Powers and Ranges in all Elemental Matter* (Pergamon Press, New York, 1977), Vol. 4.

[9] R. E. L. Green, D. H. Boal, R. L. Helmer, K. P. Jackson, and P. G. Korteling, Nucl. Phys. **A405**, 463 (1983).

[10] A. J. Koning and J. M. Akkermans, Phys. Rev C **47**, 724 (1993).

[11] H. Gruppelaar, in *Proceedings of the IAEA Advisory Group Meeting on Basic and Applied Problems on Nuclear Level Densities*, edited by M. R. Bhat (Brookhaven National Laboratory, Brookhaven, 1983), p. 143.

[12] P. Schwandt, H. O. Meyer, W. W. Jacobs, A. D. Bacher, S. E. Vigdor, M. D. Kaitchuck, and T. R. Donoghue, Phys. Rev. C **26**, 55 (1982).

[13] M. B. Chadwick, D. Phil. thesis, Oxford University, 1989; M. B. Chadwick and P. G. Young, Phys. Rev. C **47**, 2255 (1993).

[14] P. E. Hodgson, in *Proceedings of the 6th International*

Conference on Nuclear Reaction Mechanisms, edited by E. Gadioli, Varenna, 1991 (University of Milan, Varenna, 1991), p. 1.

[15] Y. Watanabe, I. Kumabe, M. Hyakutake, N. Koori, K. Ogawa, K. Orito, K. Akagi, and N. Oda, Phys. Rev. C **36**, 1325 (1987).

[16] F. D. Bechetti and G. W. Greenlees, Phys. Rev. **182**, 1190 (1969).

[17] H. Baba, Nucl. Phys. **A159**, 625 (1970).

[18] P. Demetriou, P. Kanjanarat, and P. E. Hodgson, J. Phys. G **19**, L193 (1993).

[19] W. Scobel, M. Trabandt, M. Blann, B. A. Pohl, B. R. Remington, R. C. Byrd, C. C. Foster, R. Bonetti, C. Chiesa, and S. M. Grimes, Phys. Rev. C **41**, 2010 (1990).

[20] S. M. Austin in *The (p,n) Reaction and the Nucleon-Nucleon Force*, edited by C. D. Goodman *et al.* (Plenum, New York, 1980), p. 203.